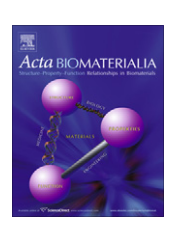
ELSEVIER

Contents lists available at ScienceDirect

Acta Biomaterialia

journal homepage: www.elsevier.com/locate/actabiomat



A novel hydrogel-collagen composite improves functionality of an injectable extracellular matrix

R. Hartwell ^a, V. Leung ^b, C. Chavez-Munoz ^a, L. Nabai ^a, H. Yang ^b, F. Ko ^b, A. Ghahary ^{a,*}

ARTICLE INFO

Article history: Received 31 December 2010 Received in revised form 13 March 2011 Accepted 25 April 2011 Available online 3 May 2011

Keywords: Injectable scaffold Collagen Polyvinyl alcohol Extracellular matrix Skin substitute

ABSTRACT

Cellular transplantation is now closer to becoming a practical clinical strategy to repair, regenerate or restore the function of skin, muscle, nerves and pancreatic islets. In this study we sought to develop a simple injectable collagen matrix that would preserve the normal cellular organization of skin cells. Three different scaffolds were created and compared: collagen–glycosaminoglycan (GAG) scaffolds, crosslinked collagen–GAG scaffolds without polyvinyl alcohol (PVA) and crosslinked collagen–GAG scaffolds containing PVA hydrogel. Importantly, all scaffolds were found to be non-cytotoxic. PVA-containing gels exhibited a higher tensile strength (P < 0.05), faster fibril formation (P < 0.001) and reduced collagenase digestion (P < 0.01) compared with other gels. Free floating fibroblast-populated, PVA-borate scaffolds resisted contraction over a 10 day period (P < 0.001). The fibroblast-populated scaffolds containing PVA demonstrated a 3-fold reduction in cellularity over 10 days compared with the control gels (P < 0.001). Multicellular skin substitutes containing PVA-borate networks display a linear cellular organization, reduced cellularity and the formation of a keratinized epidermis that resembles normal skin. In conclusion, these data underscore the multifunctionality of a simple PVA-borate-collagen matrix as an injectable composite for tissue engineering or cell transplantation.

© 2011 Acta Materialia Inc. Published by Elsevier Ltd. All rights reserved.

1. Introduction

The extracellular matrix (ECM) is a major determinant of cell survival and, ultimately, organ function. Delivery and transplantation of cells is quickly becoming recognized as a feasible clinical strategy for the repair and regeneration of organs, in part because it offers a less invasive approach. Whereas the success of skin cell and pancreatic islet transplantation are rapidly improving, clinical methods for muscle and nerve cell transplantation stand to benefit from the advent of tailored delivery systems that mimic the ECM when formed in situ [1–4].

Improved vehicles for cell delivery and encapsulation have stemmed from the principles of tissue engineering and drug delivery [1,2,5]. Tissue engineering strategies often employ collagen and glycosaminoglycan (GAG) matrices as scaffolds to mimic the tissue architecture. Simple crosslinking methods using either glutaraldehyde or 1-ethyl-3-3-dimethylaminopropyl carbodiimide:Nhydroxy-succinimide (EDC:NHS) have been exhaustively investigated as ways to improve mechanical properties and stability [2,6–9]. These strategies are in most cases utilized to fabricate solid (dry) scaffolds, however, solid scaffolds have limited application in

cell transplantation. Even as a wound coverage, preformed solid scaffolds are unable to immediately integrate with the surrounding tissue. In this regard, a liquid matrix that could integrate with the surrounding tissue upon application would be advantageous. Furthermore, as a liquid, cells could be embedded prior to casting. This is particularly important for injectable cell transplants such as pancreatic islets [1,10,11]. Unfortunately, the use of unmodified natural biomaterials has had limited success in producing useful injectable gels [2,12]. Encapsulation of cells within injectable synthetic mixtures of either pluronic acid, poly(ethylene glycol)glycol) poly(caprolactone)-poly(ethylene (PEG-PCL-PEG), poly(lactic acid) (PLA), or poly(lactic-co-glycolic acid) (PLGA) provide non-toxic, rapid gelling systems that can be modified to improve stability, but often lack a natural architecture when gelled in situ [2,5]. More recently Fitzpatrick et al. demonstrated the functionality of poly(N-isopropylacrylamide) (PNIPAAm)-collagen thermoreversible scaffolds for the delivery of retinal pigment epithelial (RPE) cells [13]. However, as with other synthetic polymers, degradation of this material may expose the tissue to potentially cytotoxic products [2]. In general, a major drawback with many new synthetic polymer systems is the length of time that is required to demonstrate safety and translate them to clinical applications.

The development of an injectable ECM using clinically approved polymers which can mimic biological structures would be

^a Burn and Wound Healing Research Laboratory, Department of Surgery, University of British Columbia, Vancouver, BC, Canada V6H 3Z6

b Advanced Fibrous Materials Laboratory, Department of Materials Engineering, University of British Columbia, Vancouver, BC, Canada V6T 124

^{*} Corresponding author. Tel.: +1 604 875 4185; fax: +1 604 875 4212. E-mail address: aghahary@interchange.ubc.ca (A. Ghahary).

advantageous for a number of medical procedures, including dermal reconstruction (as a filler), islet transplantation and as a skin graft for wound coverage. Polyvinyl alcohol is a well-known, clinically approved synthetic analog of hyaluronic acid [11,14-16]. It is an amphiphilic polymer that can crosslink to form a hydrogel in the presence of sodium borates at pH \geqslant 7 and mechanically resembles soft tissues [15,17-19]. Generally, crosslinked PVA gels are isotropic and maintain a uniform shape that has been shown to be useful for tissue engineering [20]. In this regard we hypothesized that the incorporation of PVA hydrogels within a collagen matrix would induce faster fiber formation by aiding in both hydrogen bond formation, space filling and the nucleation of collagen fibrils within a restricted environment. Although it remains to be fully understood, PVA at neutral pH provides an unsuitable substrate for cell adhesion [19,21]. We expected that the lack of cell adhesion would also restrict cell proliferation and contraction. In this study we describe the preparation of an injectable collagen scaffold containing PVA networks and evaluate its efficacy for use in tissue engineering and as an ECM for the application of skin cells.

2. Materials and methods

2.1. Collagen-glycosaminoglycan scaffolds

Three types of collagen-chondroitin sulfate scaffolds were prepared as reported by Surronen et al. with modifications [8]. Briefly summarized in Table 1, rat tail collagen type I (BD, Mississauga, Canada) was neutralized with HEPES buffer and 1 N NaOH to pH 7.0 and combined with chondroitin 6-sulfate (1:5 w/w). Crosslinked gels were prepared by crosslinking for 2 h in the dark with 0.02% (w/v) glutaraldehyde. A 2 h glycine wash was performed to deactivate remaining aldehyde groups. PVA composites were prepared by adding a mixture of 5 wt.% PVA (2.5 wt.% PVA 86, 2.5 wt.% PVA 99, 1 wt.% glycerol, Alfa Aesar, Ward Hill, MA) in $10 \times$ Dulbecco's modified Eagle's medium, pH 7.5 (Gibco®, Invitrogen, Burlington, Canada) to 0.0625 M sodium tetraborodecahydrate, pH 8.0 (Sigma, Oakville, Canada) (final concentration 0.05 wt.% sodium tetraborohydrate, 0.2% (w/v) PVA). PVA mixtures were combined with glycine washed crosslinked scaffolds and allowed to settle overnight at 4 °C prior to use. Sodium ascorbate (in filtered water pH 7.0) was added to each scaffold to a final concentration of 100 μM. Crosslinked scaffolds not containing PVA were prepared by adding sodium borate and ascorbate to the scaffold mixture following the glycine wash. Ascorbate was added to the non-crosslinked scaffolds during initial preparation. All scaffolds were prepared at the same time to a final collagen concentration of 3 mg ml⁻¹. Prepared liquid composites were stored at 4 °C and used within 1 week.

2.2. Cell populated scaffolds

Primary keratinocytes and fibroblasts were isolated from human neonatal foreskin obtained from consenting donors in accordance

Table 1 Scaffold formulation.

	Col	xCol	xCol HG
Collagen Chondroitin sulfate (in 1× PBS) Glutaraldehyde/glycine PVA (pH 7.0) Sodium borate decahydrate (pH 8) Sodium ascorbate (pH 7.0)	3 mg ml ⁻¹	3 mg ml ⁻¹	3 mg ml ⁻¹
	15 mg ml ⁻¹	15 mg ml ⁻¹	15 mg ml ⁻¹
	No	Yes	Yes
	No	No	0.2% (w/v)
	0	0.05% (w/v)	0.05% (w/v)
	100 μM	100 μM	100 μM

All concentrations are for the final product.

with the ethical guidelines set forth by the University of British Columbia. Briefly, keratinocytes were isolated from the epidermis following enzymatic digestion using 1× trypsin:EDTA (Gibco[®], Invitrogen) and Dispase (Gibco[®], Invitrogen). Fibroblasts were isolated from sections of dermis cultured in 1× DMEM supplemented with 10% fetal bovine serum (FBS) and 1% penicillin/streptomycin/ amphotericin B (Gibco®, Invitrogen). Fibroblast populated scaffolds were established at a density of 200,000-250,000 cells ml⁻¹ with the exception of the proliferation assay, which 100,000 cells ml⁻¹. Cell numbers were counted using a hemocytometer and combined with the liquid matrix in a 10% of the final gel volume suspension, producing a collagen gel of 3 mg ml⁻¹. Other cell numbers were as follows: primary keratinocytes $10^6 \, \text{ml}^{-1}$, baby hamster kidney cells (BHK) $5 \times 105 \, \text{ml}^{-1}$, HaCat 10⁶ ml⁻¹. Cells were cultured for 1 h at 37 °C prior to the addition of fresh medium (200-300 ul) specific to the cell type: keratinocytes, KSFM (Gibco[®], Invitrogen): BHK, DMEM:F12 (Gibco[®], Invitrogen).

2.3. Cell viability and morphology

Viability was assessed using a Live/Dead toxicity assay (Molecular Probes[®], Invitrogen, Carlsbad, CA). Cells (primary or cell line) were cultured for 24 h in or on top of the scaffolds (fibroblasts and BHK cultured within and keratinocytes and HaCat on top). After 24 h the scaffolds containing cells were washed three times with 1× phosphate-buffered saline (PBS), pH 7.0, and a mixture of ethidium homodimer and calcein-AM according to the manufacturer's instructions. After 30 min the scaffolds were washed three times with 1× PBS and visualized using a Zeiss Axiovert 200 M fluorescence microscope and Axiovision software. Cell counts were obtained using Image J software (NIH, Bethesda, MD). Cell morphology was visualized using wheatgerm agglutinin-conjugated Alexa Fluor 488 (Invitrogen) membrane staining of fibroblasts seeded in the collagen scaffolds 24 h after casting. Images were captured using a Zeiss Axiovert 200 M fluorescence microscope and Axiovision software.

2.4. Cellularity

Primary human fibroblasts were grown in 200 µl volume scaffolds (uncrosslinked (Col), crosslinked (xCol), crosslinked with PVA (xCol HG)) for a period of 10 days. Briefly, gels were prepared as described above and 100,000 cells ml gel⁻¹ were combined with the liquid matrix. To confirm cell totals at time 0 gels were digested with 1 U ml⁻¹ collagenase (Sigma, St. Louis, MO) and the cells subsequently counted using Trypan blue to ensure similarity (data not shown). Fibroblasts were then grown for 10 days with gel harvest on days 2, 5, 7 and 10. Gels were removed from the wells and fixed in 4% (w/v) paraformaldehyde (Sigma) for 24 h at 4 °C. Gels were then transferred to 70% ethanol and prepared for paraffin embedding. Six cross-sections (5 μm) per gel obtained from three batches of gel were de-waxed and stained with DAPI nuclear stain (Vector Labs, Burlington, Canada). Cell counts (per low power field) were obtained using a Zeiss Axioplan 2 upright fluorescence microscope.

2.5. Time to fibril formation

The time it took for collagen gels to form fibers was used to indicate casting time. Gels were prepared as described previously. Initial simple inverted test tube assays, as described previously [12], were used to estimate casting time during formulation (data not shown). Chilled gel resins (100 μ l) were aliquoted into 96-well plates (Corning, Corning, NY). DMEM containing 10% FBS and 1% penicillin/streptomycin was used as a blank. Gel resins were

chilled on ice until the absorbance measurements were taken as described previously [22,23]. Absorbance at 313 nm was recorded every 60 s over a 1 h period at 35 $^{\circ}$ C, demonstrating the rate of collagen fiber formation.

2.6. Tensile strength

Gels were cast in 5-well rectangular chamber slides (500 µl each) and incubated for 24 h at 37 °C. Tensile testing was done using a KES-G1 Micro-Tensile Tester (Kato Tech, Kyoto, Japan), with a 1 kg load cell. Prior to loading gels were dried of excess liquid using KimWipesTM (Kimberly Clark, Irving, TX) and weighed. Two pieces of KimWipeTM were then used to firmly secure the gel to the specimen holder. Gels were then stretched until breakage at a deformation rate of 0.02 cm s $^{-1}$. Tensile strength was calculated by dividing the breaking load (g) with sample width (mm) and area density (g m $^{-2}$) of the polymerized gels. For statistical purposes six batches of gels were evaluated.

2.7. Differential scanning calorimetry (DSC) and scanning electron microscopy (SEM)

The same preparation procedure was used to prepare samples for both DSC and SEM, except that gels were not fixed for DSC analysis. Collagen scaffolds (100 μ l) were cast in 96-well plates for 24 h followed by fixation in 4% formalin solution for 24 h at 4 °C. After fixation the gels were dehydrated twice for 12 h in 70% ethanol and then frozen at -80 °C prior to lyophilization. Lyophilized scaffolds were then weighed and evaluated in a Q1000 Differential Scanning Calorimeter (TA Instruments, New Castle, DE) at 5 °C min $^{-1}$ within the range 20–100 °C. SEM samples were first gold coated prior to loading inside the vacuum of a Hitachi S-3000N scanning electron microscope (Hitachi, Tokyo, Japan).

2.8. Gel contraction

Primary fibroblasts were populated within each of three collagen gels, Col, xCol and xCol HG, prepared as described previously, and cultured at 37 °C. Cell medium (DMEM containing 10% FBS and 1% antibiotics) was changed daily. Fibroblast populated collagen gels (250,000 cells ml⁻¹) were released from the plate walls 24 h after gel casting (on day 0) and allowed to contract. Images were taken on days 1, 3, 5, 7 and 10 using a Sony CyberShot H9 digital camera at a standardized range. Gel size was measured using Image J (NIH, Bethesda, MD).

2.9. Collagenase digestion

Collagen gels (100 µl) were cast in 96-well plates as described previously. Each gel was placed in 20 μl of 1× PBS (pH 7.0) containing 0.3 U of Clostridium serine peptidase A (CLSPA) purified from Clostridium histolyticum (Worthington, Lakewood, NJ). The mixture was then incubated at 37 °C for 1, 2, 6, 12 or 24 h to determine the optimal ratio of gel digestion (data not shown). Hydroxyproline measurements were carried out on digested samples (supernatant and pellets). Following digestion the gels were centrifuged three times at 15,000g for 10 min at 4 °C with a 1× PBS wash. The supernatants were separated from the pellet and recombined with 200 µl of concentrated HCl for a final concentration of 6 N. The hydroxyproline analysis was preformed as described previously [24] with minor modifications. Briefly, digested pellets were washed three times with PBS prior to adding concentrated HCl. Both pellets and supernatants were hydrolyzed for 16 h using 6 N HCl. Hydroxyproline concentrations were obtained by reading the OD at 550 nm.

2.10. Bi-layered skin substitute

Collagen gel scaffolds were prepared as described previously. Primary human fibroblasts were combined with the liquid matrix at 200,000 cells ml⁻¹ prior to casting in Transwell™ permeable supports (Corning). Fibroblast populated gels were then incubated for 48 h at 37 °C in DMEM containing 10% FBS and 1% antibiotic (Gibco®, Invitrogen). Primary human keratinocytes were cultured to 60% confluence in KSFM containing bovine pituitary extract (BPE), epidermal growth factor (EGF) and 1% antibiotic (Gibco®, Invitrogen). After 48 h keratinocytes (1×10^6 cells) were seeded on top of the cultured gel scaffolds and the medium was changed to 49% DMEM, 49% KSFM with 1% FBS, and 1% antibiotic (50/50 medium) as previously described [25]. The medium was changed after 24 h and after 36 h the gels were raised to the liquid air interface in order to differentiate keratinocytes. The gels were cultured in a Transwell™ (with a dry surface) for 10 days (5% CO₂) with 50/ 50 medium containing 100 µM ascorbic acid. The medium was changed daily. After 10 days the bi-layered skin substitutes were removed from the Transwell™ and cast in a 1% agar gel. The gel was then fixed in 4% formalin for 24 h. Paraffin embedded sections (5 μm) were stained with hematoxylin and eosin (H&E) and images were captured using a Zeiss Axioplan 2 (Carl-Zeiss, North York, Canada) upright microscope.

2.11. Statistics

The number of repeats represents different batches of gels. Experimental results were evaluated using analysis of variance (ANOVA) with a post hoc Tukey test. Statistical significance was estimated with an α value of \leq 0.05. Measurements are reported as means \pm standard deviation.

3. Results

3.1. Casting time

Two key characteristics of an injectable ECM are rapid gelation and immobilization of cells. Our goal is to create a system that could be applied through injection or topically within a working window of 15 min prior to solidification. Fibril formation in vitro, through entanglement of the collagen coiled–coiled structure, is the final step of collagen gelation. As such, acellular liquid collagen solutions, either uncrosslinked (Col, Fig. 1A), crosslinked (xCol, Fig. 1B) or crosslinked containing PVA–borate hydrogels (xCol HG, Fig. 1C), were evaluated for their rate of fibril formation. Time to fibril formation is calculated by the time to half maximum absorbance at 313 nm. The lag time ($t_{\rm lag}$) is described as the time difference between the time of the intersect between the slope (dA/dt) and the initial baseline absorbance ($A_{\rm i}$) [22], represented by the equation:

$$t_{\text{lag}} = (A_{\text{i}} - b)/(dA/dt)$$

where b is the intercept of the line (dA/dt).

The results shown in Fig. 1D suggest that PVA–borate gels (xCol HG) require less than half the time to form (P < 0.001) with a reduced lag time to initiate fibril formation compared with other gels (P < 0.001). As described in Supplementary Table S1, the time to initiate fibril formation when heated from 4 °C to 37 °C is 13.65 min (819.1 ± 153.7 s), with fibrils being formed after 16.3 min (978 ± 268.4 s). Although both crosslinked gels with and without PVA–borate undergo shorter transitions to complete fibril formation, both the lag time and the time to half maximum absorbance for crosslinked gels without PVA–borate (1556.6 ± 203.9 and

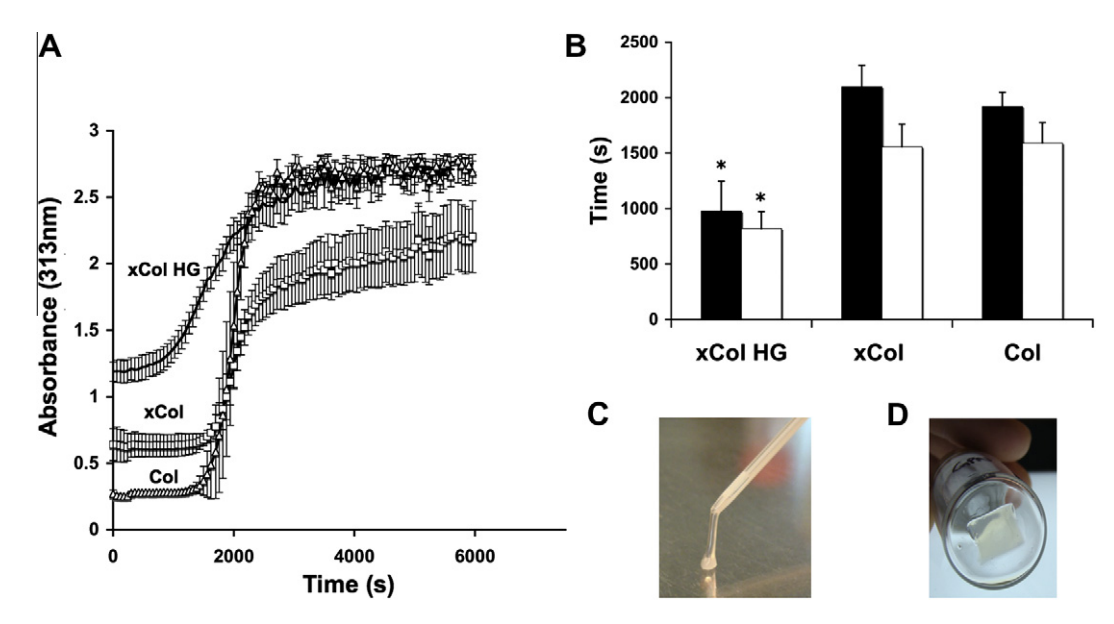


Fig. 1. Time to fibril formation and gelation of collagen–GAG scaffolds. (A, B) Three collagen gels were prepared on ice and maintained at 4 °C: collagen–GAG (COI), crosslinked collagen–GAG (xCoI) and crosslinked collagen–GAG containing PVA–borate networks (xCoI HG). To measure turbidity and rate of fibril formation gels were incubated from 4 °C to 37 °C and absorbance was measured every 30 s at 313 nm. DMEM (cell medium), DMEM with borate and DMEM containing PVA–borate were used as the respective blanks. (A) Turbidity shift of collagen scaffolds. (B) Time to fibril formation ($t_{1/2 \text{ max}}$ absorbance) (solid bars) and lag time to initiate fibril formation (open bars). (C) Ejected xCoI HG scaffold after casting in a catheter tube at 37 °C for 7 min. (D) xCoI HG scaffold after casting in a rectangular tray at 37 °C. (n = 9, P < 0.05) *P < 0.05.

 2096 ± 196.4 s) were not significantly different from uncrosslinked collagen gels (1589.2 \pm 186.9 and 1920 \pm 128.6 s).

3.2. Tensile strength

Matrix strength is integral in predicting its functionality as an engineered tissue. Although it is well known that crosslinking of collagen increases the matrix strength, we were interested in whether the addition of PVA-borate networks at a dilute concentration had any effect on the tensile properties of the matrix. Stress-strain curves of collagen gels, shown in Fig. 2A-C, depict good agreement among different batches and are consistent with previous findings [9,26]. The results demonstrate that the maximum strain at break was statistically similar among the uncrosslinked $(8.4 \pm 1.2\%)$, crosslinked $(12.5 \pm 7.02\%)$ and crosslinked with PVA-borate $(8.0 \pm 1.3\%)$ systems (Supplementary Table S2). However, the tensile modulus (Y (Δ stress/ Δ strain)) of the crosslinked collagen containing PVA-borate (1.414 ± 0.5015 MPa) was significantly greater than that of the crosslinked collagen (P = 0.03) and uncrosslinked collagen (P < 0.001). Furthermore, the maximum stress at break was also significantly greater in the xCol HG $(0.074 \pm 0.0498 \text{ N m}^{-2})$ system compared with uncrosslinked collagen (0.014 \pm 0.0056 N m⁻², P = 0.01).

3.3. Cell viability and morphology

Although glutaraldehyde crosslinked collagen matrices have been used and studied extensively, it was essential to determine whether PVA–borate systems exhibit toxicity. As there is the potential for this scaffold to be used as a cell delivery matrix, as a wound coverage or via injection we assessed and compared the toxicity across a range of cell lines and primary cells. As shown in Fig. 3, primary human fibroblasts and keratinocytes, two key cellular components of skin, exhibited $86 \pm 12\%$ and $78.8 \pm 3.2\%$ viability, respectively, when cultured in or on the xCol HG composite. Similarly, BHK cells and the HaCat cell line remained $79.6 \pm 9.7\%$ and $84.8 \pm 4\%$ viable when cultured on the xCol HG composite scaffolds. With the exception of primary human

keratinocytes, cell viability on crosslinked scaffolds was similar to uncrosslinked scaffolds. Primary human keratinocytes cultured on either crosslinked scaffold were on average 12% less viable (P < 0.001) than those cultured on uncrosslinked collagen. The morphology of fibroblasts cultured inside the xCol HG gels for 24 h (Fig. 3C) displayed a linear pattern compared with those cultured in either uncrosslinked or crosslinked collagen gels. Interestingly, cell spreading in both the uncrosslinked and crosslinked gels was random, whereas in xCol HG gels it appeared to be unidirectional relative to a given location (i.e. plane) in the scaffold.

3.4. Cellularity

High cellularity is a marker of tissue fibrosis. Control of fibroblast proliferation can be beneficial to reduce the degree of postwound scarring and capsular contracture around implanted materials. It has been established that cells grown in a collagen gel (three-dimensional, 3-D) exhibit reduced cellularity than those cultured on a plate surface (two-dimensional, 2-D). In order to evaluate cellularity in these collagen systems paraffin embedded gels were sectioned and analyzed under a fluorescence microscope in a low power field (LPF). The results in Fig. 4B describe a marked increase in cellularity from day 6 to day 10 in uncrosslinked scaffolds. As of day 10 xCol HG scaffolds have 5-fold fewer cells per LPF (P < 0.001) compared with uncrosslinked collagen–GAG gels. Furthermore, the addition of PVA–borate hydrogels to the scaffold significantly reduced cellularity (23 ± 4 cells per LPF) compared with the xCol gels (35 ± 5 cells per LPF, P < 0.001).

3.5. Resistance to contraction

Hallmark determinants of contracture are a high cellularity and a reduction in gel strength [27]. In order to evaluate whether xCol HG could mitigate cell-mediated contraction cast gels were released from the plate surface and the surface area was measured daily over 10 days. As shown in Fig. 5A uncrosslinked collagen gels rapidly underwent contraction to nearly half the original size within 1 day of being released from the plate surface (P < 0.001). Both

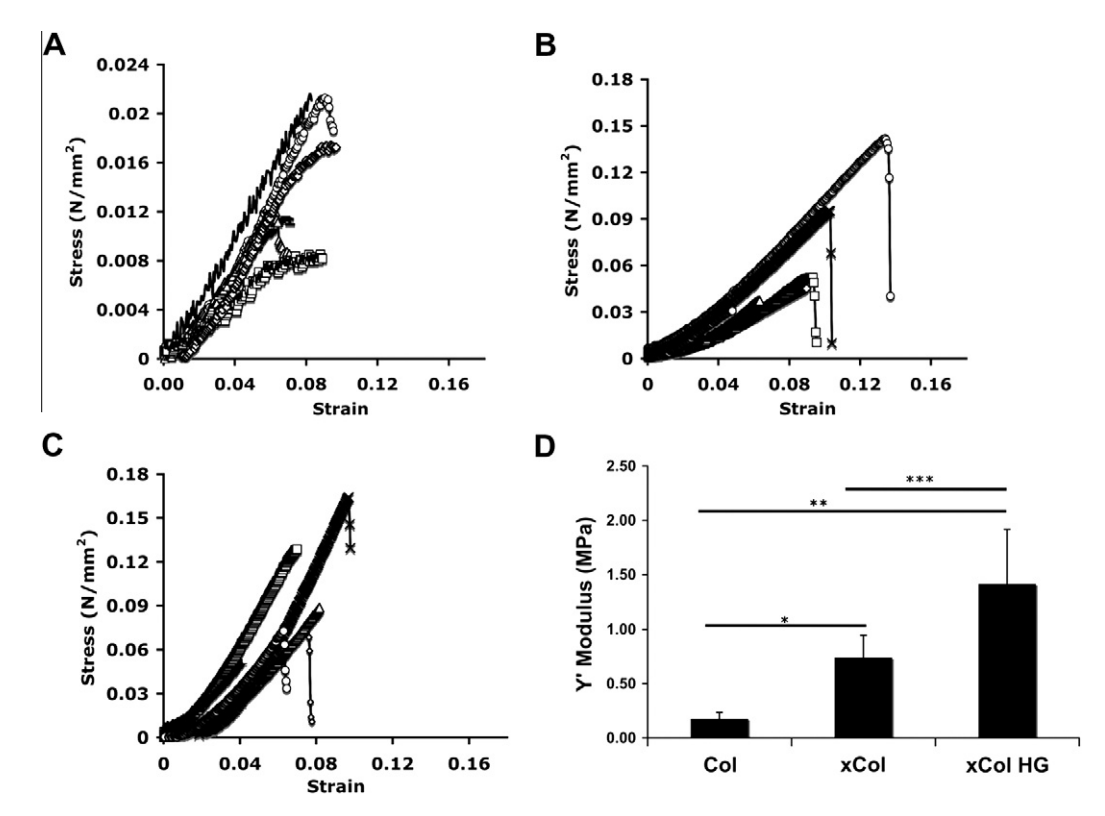


Fig. 2. Mechanical properties of hydrate collagen–GAG gels. Three collagen gels were cast in 500 μ l rectangular wells at 37 °C for 24 h prior to testing: collagen–GAG (COI), crosslinked collagen–GAG (xCoI) and crosslinked collagen–GAG containing PVA–borate networks (xCoI HG). Following incubation gels were weighed and loaded on the tensile mounts. Gels were then stretched until breaking point at a rate of 0.1 cm s⁻¹. The results represent six different batches of gel. Strain (σ) was calculated as a function of area density and Young's modulus as the slope of the curve (ε/σ). (A–C) Stress versus strain curves for six different trials of each collagen scaffold: (A) Col, (B) xCol and (C) xCol HG. (D) Average Young's modulus for six batches of collagen scaffold. The error is represented as the standard deviation. (P < 0.05) *P = 0.03, ***P < 0.001, ***P

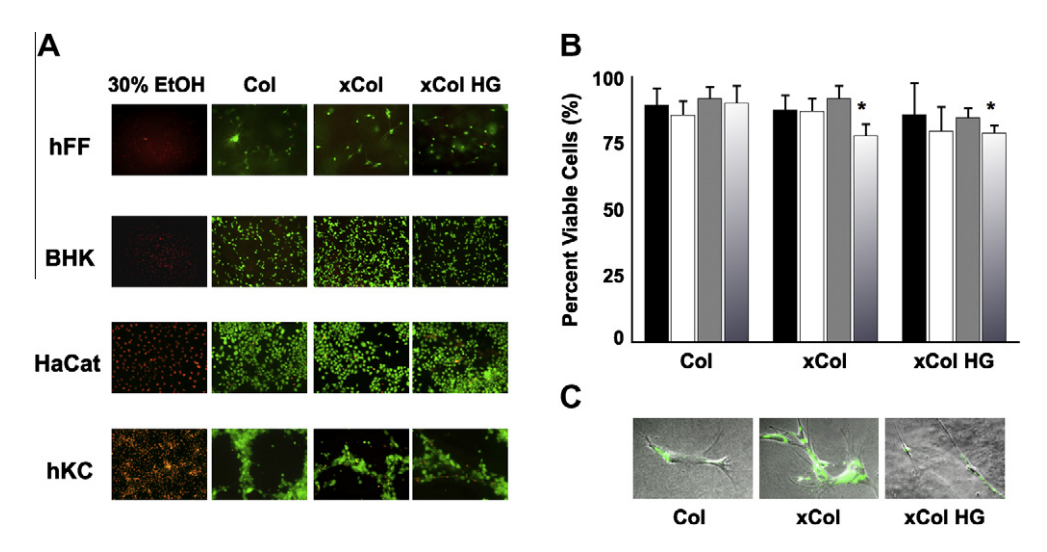


Fig. 3. Viability and morphology of cells cultured in or on collagen–GAG scaffolds. Three collagen gels were prepared at 4 °C: collagen–GAG (Col), crosslinked collagen–GAG (xCol) and crosslinked collagen–GAG containing PVA–borate networks (xCol HG). (A, B) Primary human fibroblasts (hFF, solid bars), baby hamster kidney cells (BHK, open bars), a human keratinocyte cell line (HaCat, grey bars), and primary human keratinocytes (hKC, gradient bar) were evaluated for viability after 24 h on each of the different scaffolds. HaCat, hKC and BHK were all cultured on top of the collagen scaffolds, whereas hFF were cultured within them. Cells were stained with a mixture of calcein AM (green, viable) and ethidium homodimer (red, dead) to indicate cytotoxicity of the scaffolds. 30% ethanol was used as a negative control. Cell numbers were obtained from low magnification field images using Axiovision lite software. Cell numbers and standard deviations reflect the entire population of cells in triplicate (three batches of gels). (C) Phase contrast micrograph of fibroblasts within xCol HG gels. Fibroblasts were pretreated with a fluorescent dye–*n*-glutenin membrane label (green) to depict cell morphology and surface area inside the cast scaffold after 24 h. (*n* = 3, *P* < 0.05) **P* = 0.045.

crosslinked gels were able to mitigate contraction over a 3 day period (>75% original size), however, following day 3 the xCol scaffolds significantly reduced in size (day 5 P < 0.0001; day 7 P = 0.004; day 10 P < 0.0001) relative to xCol HG. On day 5 the uncrosslinked scaffolds had reduced to near their minimum size

at $25 \pm 6\%$ of their original surface area, whereas the xCol HG scaffolds were still $91 \pm 5\%$ of their original surface area (Fig. 5B). Furthermore, by day 10 the xCol HG scaffolds were able to resist contracture by $57 \pm 7.2\%$, compared with the xCol scaffolds at $38 \pm 9.6\%$ (P < 0.001).

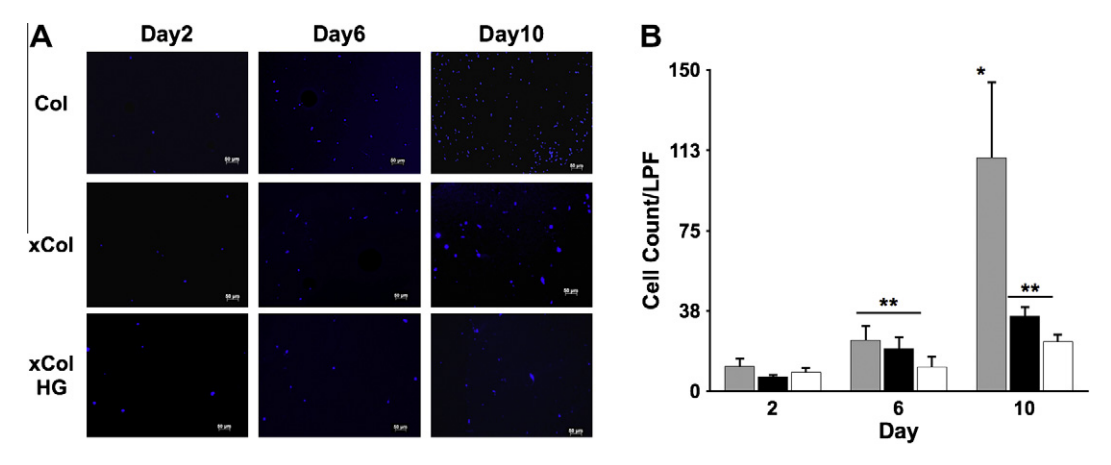


Fig. 4. Fibroblast cellularity when cultured within collagen–GAG scaffolds over a 10 day period. Again, three collagen gels were prepared at 4 °C: collagen–GAG (Col, grey bar), crosslinked collagen–GAG (xCol, closed bar) and crosslinked collagen–GAG containing PVA–borate networks (xCol HG, open bar). Primary fibroblasts were incorporated within the gel resin prior to casting at 37 °C. Gels were washed and fixed in 4% paraformaldehyde for 12 h prior to paraffin embedding on days 2, 6 and 10. Sections were dewaxed and stained with DAPI nuclear stain in order to count total cell numbers in low power field (LPF). Six sections were counted from three different batches of gels. (A) Representative low power images of DAPI stained gel sections. (B) Average cellularity of scaffolds on days 2, 6 and 10. (n = 3, P < 0.05) *P = 0.01, **P < 0.001 (scale bar 50 μM).

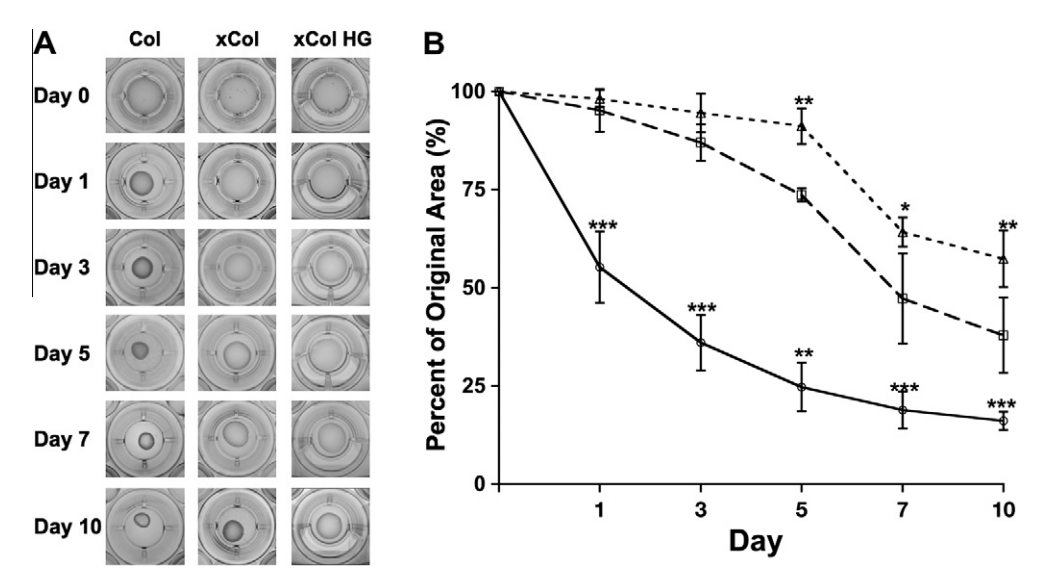


Fig. 5. Contraction of free floating fibroblast populated collagen–GAG scaffolds (FFPC). Primary fibroblasts were cultured within each of three collagen gels and cultured at 37 °C: collagen–GAG (Col, open circle), crosslinked collagen–GAG (xCol, open square) and crosslinked collagen–GAG containing PVA–borate networks (xCol HG, open triangle). Cell medium (DMEM containing $10 \times FBS$ and $1 \times$ antibiotics) was changed daily. FFPC were released from the plate walls on day 0 and allowed to float. (A) Contraction images of FFPC over the course of 10 days. (B) Resistance to gel contraction as marked by the per cent original gel on days 1, 3, 5, 7 or 10, where day 1 represents 24 h following release of the scaffold from the plate walls. (n = 3 batches of gel, P < 0.05) ***P < 0.001, **P < 0.001, **P < 0.05.

3.6. Thermal stability

Thermal stability and heat capacity is not only important for "shelf-life" but also as an indicator of molecular bonding. It has separately been established that PVA and collagen exhibit distinct thermal properties, and that a combination of these polymers can alter material characteristics [16]. Lyophilized collagen gels were evaluated using DSC at a rate of 5 °C min⁻¹. Representative DSC isotherms found in Fig. 6A-C show that crosslinking of collagen eliminates the glass transition observed with uncrosslinked collagen. The heat loss by crosslinked collagen (Fig. 6B) is much greater than that by uncrosslinked collagen approaching its crystallization point at 90 °C (consistent with both scaffolds). However, the addition of PVA-borate (Fig. 6C) (even at 0.2%) distinctly changes the isotherm of the crosslinked scaffold (Fig. 6B). The heat capacity is notably increased at a $T_{\rm g}$ of 30 °C through to a second peak at 45 °C in xCol HG with no evident sign of crystallization at temperatures under 100 °C (Fig. 6C). It is known that PVA has a $T_{\rm g}$ of 85 °C, which may explain the slight change in heat flow at around 90 °C [28]. The homogeneity of the heat flow curve suggests that addition of the PVA-borate hydrogel produces a stable polymer network.

3.7. Resistance to enzyme degradation

It has been previously established that the level of matrix metalloproteinases (MMP), matrix degrading enzymes, increases when fibroblasts are cultured within a collagen gel. In order to investigate whether the addition of a PVA-borate hydrogel to the scaffold could mitigate enzymatic degradation acellular gels were incubated in the presence of pure collagenase (CLSPA) for 24 h. Results were quantified by measuring the hydroxyproline content. $80 \pm 0.4\%$ (P < 0.001) of the uncrosslinked collagen was digested (Fig. 6D). Interestingly, as is evident from the hydroxyproline content, PVA-borate hydrogels exhibited reduced degradation

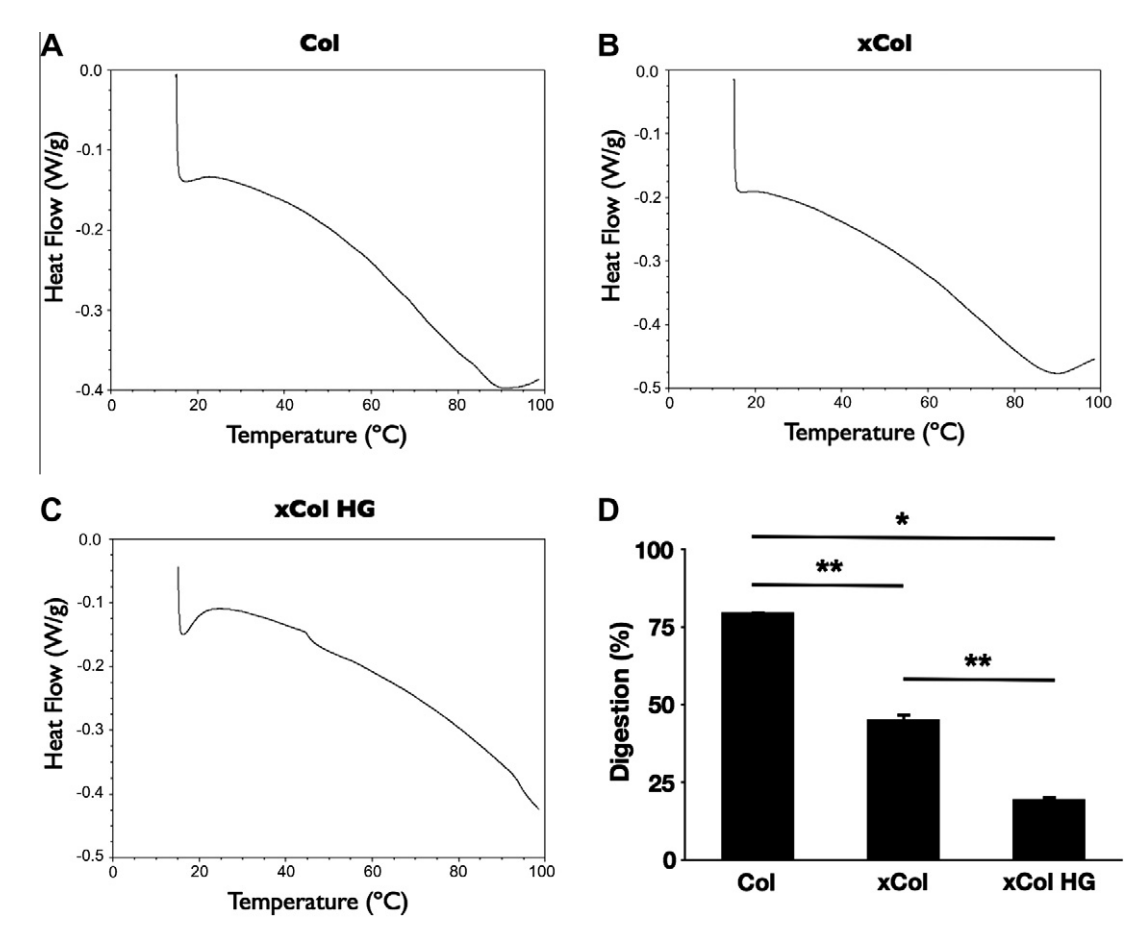


Fig. 6. Thermal and enzymatic stability of collagen–GAG scaffolds. Three collagen gels were prepared at 4 $^{\circ}$ C and cast at 37 $^{\circ}$ C: collagen–GAG (Col), crosslinked collagen–GAG (xCol) and crosslinked collagen–GAG containing PVA–borate networks (xCol HG). (A–C) Differential scanning isotherms representative of different lyophilized scaffolds. The temperature was raised at 5 $^{\circ}$ C min⁻¹, within the range 20–100 $^{\circ}$ C. (D) Hydroxyproline content of the digested supernatant calculated as a percentage of the total gel content. (n = 3, P < 0.05) **P = 0.01, *P < 0.001.

 $(19.5 \pm 1\%)$ compared with those of both crosslinked $(45.2 \pm 2\%)$ and uncrosslinked collagen (above) after 24 h.

3.8. Scanning electron microscopy (SEM)

Pore size and fiber diameter are key modulators of cell physiology in a collagen scaffold. SEM imaging in Fig. 7 reveals a distinct network of fibers in the crosslinked collagen scaffolds (Fig. 7B and E) resembling a mesh, unlike the larger fibers found in the uncrosslinked gels (Fig. 7A and D). Unexpectedly, addition of the PVA-borate hydrogel to the crosslinked networks created a heterogeneous network of channels, which appeared to be separated by a thin film rather than fibers (Fig. 7C and F). The topography of the xCol HG network suggests that it contains fibrous elements that are filled with PVA-borate (or glycosaminoglycan), similar to previous findings [16,19,21,29].

3.9. Engineered skin substitute (ESS)

The development of a liquid matrix system for cell delivery may be advantageous for application as a skin substitute. In vitro morphology of cells cultured in the xCol HG composite ESS showed a linear arrangement, which differed from the random attachments observed in either uncrosslinked or crosslinked collagen scaffolds. In order to evaluate the architecture of skin substitutes prepared over a 14-day period using both primary fibroblasts and keratinocytes paraffin embedded sections of ESS were mounted on slides and analyzed using H&E staining. The results demonstrate that a

similar linear morphology to the fibroblasts depicted in Fig. 3C was also achieved in the xCol HG ESS (Fig. 8C). On the other hand, cellular organization was random in both of the other ESS. Furthermore, the cellularity was also markedly less in xCol HG (Fig. 8C) and resembled the cross-section of full thickness skin. Finally, it was also evident that the thickness of both crosslinked scaffolds (Fig. 8A and B) was consistent across the entire section, whereas in the uncrosslinked scaffolds the middle of the gel was thinner than at the edge.

4. Discussion

Cell transplantation offers significant advantages over solid organ transplants for tissue repair and regeneration as a less invasive approach with potentially reduced immunosuppression [1,30]. One of the main hurdles for cell transplantation is the development of a viable injectable cell matrix system that will integrate with surrounding tissues while mitigating fibrotic responses. Several approaches to creating injectable scaffolds have employed crosslinking reagents, as well as modified synthetic and natural polymers that undergo crosslinking in situ. In this study we chose to use glutaraldehyde as a rapid, well-established collagen crosslinker. Notably, we found our crosslinked gels to be non-toxic to both cell lines and primary cells. Although primary fibroblasts were used throughout the study, the viability of primary keratinocytes cultured on the gels was also evaluated in order to asses the usefulness of the scaffolds as skin substitutes. Furthermore, the viability of BHK cells (an epithelial cell type) and the HaCat

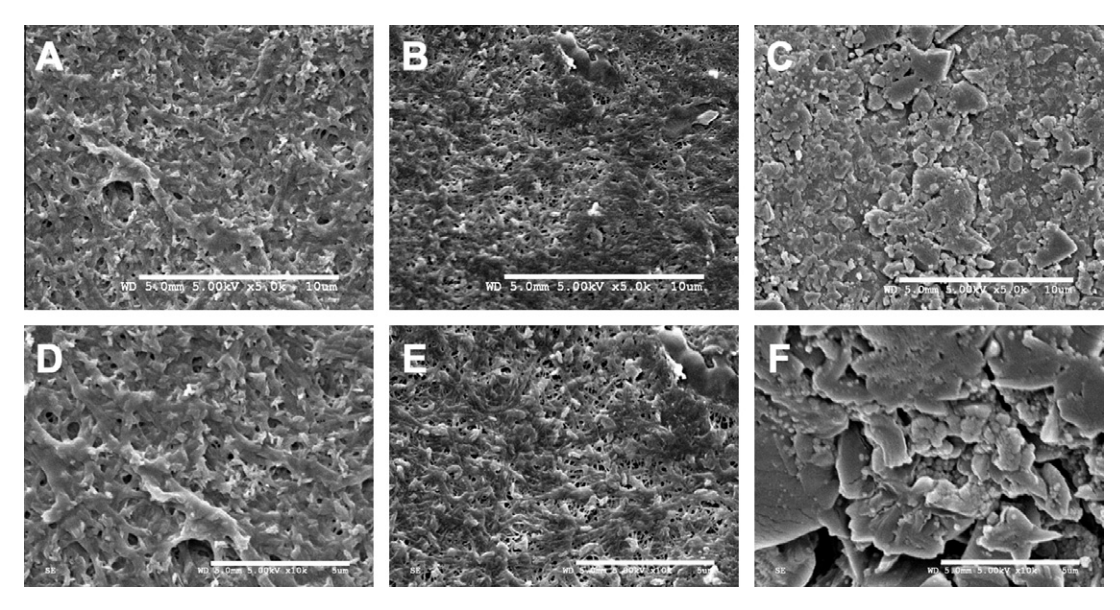


Fig. 7. SEM micrographs of three different collagen gels: (A, D) collagen–GAG, (B, E) crosslinked collagen–GAG and (C, F) crosslinked collagen–GAG containing PVA–borate networks. Gels were cast at 37 °C, dehydrated in 70% ethanol and freeze dried at -80 °C prior to gold plating. Images (A–C) 5 kV \times 5 k and (D–F) 5 kV \times 10 k. Scale bars 10 μ m (A–C) and 5 μ m (D–F).

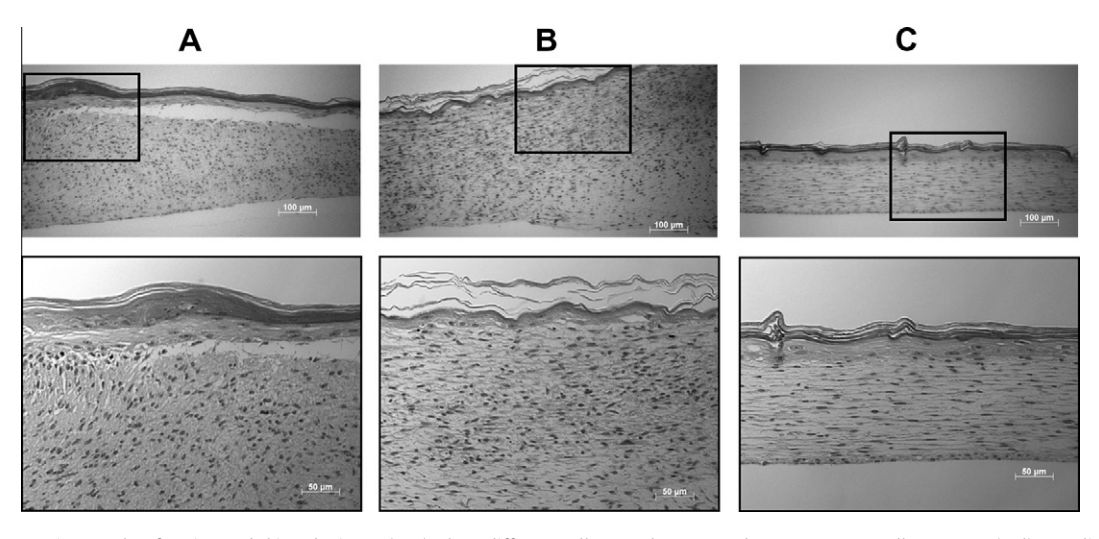


Fig. 8. Phase contrast micrographs of engineered skin substitutes (ESS). Three different collagen gels were used to prepare ESS: collagen–GAG (Col), crosslinked collagen–GAG (xCol) and crosslinked collagen–GAG containing PVA–borate networks (xCol HG). First, primary fibroblasts were combined with gel resin prior to casting in a permeable support for 48 h at 37 °C. After 48 h primary keratinocytes were seeded on top of the scaffolds and the medium was changed to 50/50 DMEM/KSFM as described in Section 2. After 36 h the medium was lowered to expose the gel liquid interface and allow keratinocytes to develop over a 14 day period. Images represent H&E stained sections from paraffin embedded ESS. Scale bars 100 μm (A–C) and 50 μm (D–E).

(immortalized keratinocyte) cell line were included in our investigation to ensure that a variety of cells could be grown in our scaffold. Importantly, all cultured cells remained viable in the presence of polyvinyl alcohol-borate in or on any of the collagen–GAG scaffolds.

PVA is a neutral polymer that easily undergoes hydrogen bonding under physiological and basic conditions [17,18,21,31]. The formation of a gel as a result of hydrogen bonding is most pronounced in the presence of sodium borates. The bonding between borate and PVA is well known to cause rapid gelation under concentrated conditions [18]. In this study we added a dilute PVA-borate mix to collagen–GAG resins in order to produce a rapidly formed injectable ECM. Using a simple inverted tube assay [15,32] we were able to observe the crosslinking of collagen at 37 °C in less than 10 min (data not shown). Although a solid gel may form within 10 min, the formation of fibrils (i.e. complete gelation) will take longer. Crosslinked collagen scaffolds containing the PVA-borate hydrogel (xCol

HG) showed a significantly increased rate of fibril formation (16.3 min), as well as a reduction in the lag time. This could be explained as the result of hydrogen bonding between PVA-borate and collagen complexes that increases the viscosity and enhances the nucleation of collagen fibers at 37 °C [33,34]. Bonding between PVA and collagen was previously shown to create stronger biomaterials [16]. In vivo collagen provides strength and toughness. Hyaluronic acid (HA) is an abundant tissue glycosaminoglycan providing lubrication and resiliency. It was thought that the addition of a PVA-borate hydrogel similar to HA would not only increase the strength but also elasticity. When xCol HG demonstrated a significantly higher tensile strength (Y) (1.414 ± 0.5015 MPa) than either of the control gels the ultimate elasticity was not improved. One possibility is that there is more extensive bonding between the collagen and PVA networks at dilute PVA concentrations, which requires a greater force per unit area of strain [34]. Thus, once the breaking force is reached the bond energies are broken and the gel tears. The DSC results (Fig. 6) suggest that there is a more extensively bonded (hydrogen) network in the PVA-borate and collagen-GAG crosslinked composites compared with the other two scaffolds, as marked by an increased heat capacity. These data suggest that intramolecular bonding between the polymer species (PVA and collagen) may have an additive effect in improving the strength of the gel [35]. In comparison, the elastic strength of the actual dermis (in vivo and ex vivo) has been found to be in the range 0.6-5 MPa, with rat dermis slightly less at 0.4 MPa and simple dermal equivalents of the order of 8-10 kPa [36-38]. Normal loads (using indentation) have recently been reported to be in the range 1-10 kPa [39]. In actual dermis it was shown that below a 10% strain rate the mechanical properties of the dermis differ significantly from at higher strain rates, which may be due to the presence of elastin-unwinding and adhesion of proteoglycans. Where patient age, matrix composition, hydration, relative humidity and the method can alter these values considerably, our results demonstrate that even in the absence of cells the hydrogel-containing injectable scaffold (once formed) can exhibit comparable mechanical stiffness to actual dermis. More importantly, these data demonstrate that the composite collagen matrix confers a greater tensile strength compared with crosslinked and uncrosslinked scaffolds, and may in part explain the resistance to contraction of free floating gels.

Free floating collagen gels have a tendency to contract when populated with fibroblasts [27]. Contraction in vitro is a function of both the mechanical force required to cause contraction and the total number of fibroblasts needed to apply a given force [40]. Thus it is reasonable to suggest that a stiffer material will require more fibroblasts to produce contraction. Our results suggested a significant decrease in proliferation from day 5 to day 10 in both crosslinked gels compared with the uncrosslinked gel. The addition of PVA further reduced proliferation from day 6 to day 10 as the total number of cells on day 10 was significantly less in xCol HG than that in xCol gel. Previously PVA composites were found to be inadequate growth substrates for fibroblasts, as suggested by the possible lack of adhesion points. In our study we used a significantly lower amount of PVA within our composites. whereby cells could adhere. Cell morphology (Fig. 3) in the presence of PVA-borate was visibly different, maintaining a spindle shaped morphology. The amount of PVA (0.2% w/v) was less than the amount of HA used in other gel composites, and was also the upper limit that could be applied without causing premature gelation (data not shown) [41]. Together, the improved tensile strength and reduced proliferation observed in our composite gels suggests that they would provide greater resistance to contraction compared with either crosslinked or uncrosslinked gels. The significant difference in contraction between the crosslinked collagen gels and those containing PVA-borate occurred after day 3. In fact, with the exception of day 7, scaffolds containing PVA significantly resisted contraction from day 5 to day 10 (compared with crosslinked gels without PVA) and maintained nearly 60% of their original size at the end of the study. Interestingly, these data follow the same trend observed in cell counts over the same period (Fig. 4).

Within a short period of time fibroblasts are able to remodel collagen scaffolds, causing them to degrade. Fragmented collagen and GAG have been shown to induce proliferative, fibrotic and immune responses [40]. As a cell transplant delivery system we were interested to learn if this composite system would be able to withstand specific degradation by collagenase. *Clostridium* serine peptidase A is the most purified *Clostridium* collagenase responsible for initiating digestion by unwinding and cleaving collagen, ultimately exposing it to other proteolytic enzymes [42]. The hydroxyproline content in digested samples demonstrated that the PVA-borate gels were more resistant to degradation than either of the other gels. Similar to previous findings, crosslinked collagen was more

resistant than uncrosslinked collagen. One explanation for these observations is that in addition to the glutaraldehyde crosslinks, the entanglement of PVA-borate networks among collagen fibrils further inhibited enzymatic attack [35]. In support of this explanation, SEM images of the PVA-borate composites, unlike the Col and xCol gels, show a lack of any fibers, and the rather film formed crevasses. Compared with SEM images of other PVA-borate mixtures, thin films in the void space between and around the crosslinked collagen bundles may in part explain the absence of fibers in the xCol HG images [15]. Interestingly the "crack and crevasse" appearance in Fig. 7F, is similar to the SEM topography of acellularized pig and human dermis [43,44].

Skin substitutes, as a cell transplant, are now becoming a more attractive option for the treatment of severe burns and chronic wounds. When we compared the histology of skin substitutes created using either uncrosslinked, crosslinked or crosslinked PVAborate containing collagen-GAG scaffolds it was found that those containing PVA were most similar to skin. Cellularity, cell morphology and even the skin layers (dermis and epidermis) were more consistent with the normal anatomy. Furthermore, the evident reduction in cell proliferation within the skin substitute containing PVA-borate (Fig. 8) was also consistent with our findings in Fig. 4. Interestingly, fibroblasts maintained a linear shape (similar to the morphology found in Fig. 3) that may be caused by a restrictive environment created by the PVA-borate network. Ultimately this could produce a niche in which fibroblasts can survive but not overgrow. The extensive hydrogen bonding and, perhaps, charge neutralization as a result of PVA-borate networks could reasonably create regions that are unfavorable for cell adherence. Further studies are required to better understand the morphological response of fibroblasts cultured within the PVA-borate containing skin substitutes. The use of injectable gels has the potential to improve the success of skin cell transplants as in situ forming skin substitutes. At present there exist a variety of materials in which to deliver cells. Refinement of these injectable systems is needed to produce a matrix that, once gelled, assumes the desired architecture, similar to solid, preformed scaffolds.

5. Conclusion

Our study evaluated the formulation of a simple, injectable collagen–GAG ECM containing networks of PVA–borate. Specifically, we demonstrated that the incorporation of PVA–borate networks was not only needed for timely gelation of the ECM, but also improved the architecture and mechanical properties. While high cellularity and contracture is usually associated with fibrosis, these gels demonstrated the potential to dampen cell proliferation and contraction, without compromising cell viability. Taken together, the improved functionality of our simple PVA–borate containing collagen system warrants further investigation for use in cell transplantation as a dermal substitute or injectable matrix.

6. Conflict of interest

The authors state no conflict of interest.

Acknowledgements

This study was supported by Canadian Institutes of Health Research (CIHR). R.H. holds a University of British Columbia Graduate Fellowship, the CIHR Transplantation Training Scholarship and the CIHR-Skin Research Training Centre Studentship Award. Special thanks go to Dr. Yunuan Li, Dr. Reza B. Jalili and Alexa Verspoor for their contributions to this work.

Appendix A. Figures with essential colour discrimination

Certain figures in this article, particularly Figures 1, 3, and 4, are difficult to interpret in black and white. The full colour images can be found in the on-line version, at doi:10.1016/j.actbio.2011.04.024.

Appendix B. Supplementary data

Supplementary data associated with this article can be found, in the online version, at doi:10.1016/j.actbio.2011.04.024.

References

- [1] Turner R, Gerber D, Reid L. The future of cell transplant therapies: a need for tissue grafting. Transplantation 2010;90(8):807–10.
- [2] Coutu DL, Yousefi AM, Galipeau J. Three-dimensional porous scaffolds at the crossroads of tissue engineering and cell-based gene therapy. J Cell Biochem 2009;108(3):537–46.
- [3] Okada M, Payne TR, Oshima H, Momoi N, Tobita K, Huard J. Differential efficacy of gels derived from small intestinal submucosa as an injectable biomaterial for myocardial infarct repair. Biomaterials 2010;31(30):7678–83.
- [4] Walsh S, Midha R. Practical considerations concerning the use of stem cells for peripheral nerve repair. Neurosurg Focus 2009;26(2):E2.
- [5] Van Tomme SR, Storm G, Hennink WE. In situ gelling hydrogels for pharmaceutical and biomedical applications. Int J Pharm 2008;355(1/2):1–18.
- [6] Duan X, McLaughlin C, Griffith M, Sheardown H. Biofunctionalization of collagen for improved biological response: scaffolds for corneal tissue engineering. Biomaterials 2007;28(1):78–88.
- [7] McLaughlin CR, Acosta MC, Luna C, Liu W, Belmonte C, Griffith M, et al. Regeneration of functional nerves within full thickness collagen– phosphorylcholine corneal substitute implants in guinea pigs. Biomaterials 2010;31(10):2770–8.
- [8] Suuronen EJ, McLaughlin CR, Stys PK, Nakamura M, Munger R, Griffith M. Functional innervation in tissue engineered models for in vitro study and testing purposes. Toxicol Sci 2004;82(2):525–33.
- [9] Powell HM, Boyce ST. EDC cross-linking improves skin substitute strength and stability. Biomaterials 2006;27(34):5821–7.
- [10] Jalili RB, Forouzandeh F, Rezakhanlou AM, Hartwell R, Medina A, Warnock GL, et al. Local expression of indoleamine 2,3 dioxygenase in syngeneic fibroblasts significantly prolongs survival of an engineered three-dimensional islet allograft. Diabetes 2010;59(9):2219–27.
- [11] Qi Z, Shen Y, Yanai G, Yang K, Shirouzu Y, Hiura A, et al. The in vivo performance of polyvinyl alcohol macro-encapsulated islets. Biomaterials 2010;31(14):4026–31.
- [12] Zheng L, Ao Q, Han H, Zhang X, Gong Y. Evaluation of the chitosan/glycerol-beta-phosphate disodium salt hydrogel application in peripheral nerve regeneration. Biomed Mater 2010;5(3):35003.
- [13] Fitzpatrick SD, Jafar Mazumder MA, Lasowski F, Fitzpatrick LE, Sheardown H. PNIPAAm-grafted-collagen as an injectable, in situ gelling, bioactive cell delivery scaffold. Biomacromolecules 2010;11(9):2261–7.
- [14] Chiellini E, Cinelli P, Grillo Fernandes E, Kenawy el RS, Lazzeri A. Gelatin-based blends and composites. Morphological and thermal mechanical characterization. Biomacromolecules 2001;2(3):806–11.
- [15] Cho SH, Lim SM, Han DK, Yuk SH, Im GI, Lee JH. Time-dependent alginate/ polyvinyl alcohol hydrogels as injectable cell carriers. J Biomater Sci Polym Ed 2009;20(7/8):863–76.
- [16] Ficai M, Andronescu E, Ficai D, Voicu G, Ficai A. Synthesis and characterization of COLL-PVA/HA hybrid materials with stratified morphology. Colloids Surf B Biointerfaces 2010;81(2):614–9.
- [17] Valentin JL, Lopez D, Hernandez R, Mijangos C, Saalwachter K. Structure of poly(vinyl alcohol) cryo-hydrogels as studied by proton low-field NMR spectroscopy. Macromolecules 2009;42(1):263–72.
- [18] Ani Idris NAMZ, Suhaimi MS. Immobilization of baker's yeast invertase in PVAalginate matrix using innovative immobilization techniques. Process Biochem 2008;43:331–8.
- [19] Ramires PA, Milella E. Biocompatibility of poly(vinyl alcohol)-hyaluronic acid and poly(vinyl alcohol)-gellan membranes crosslinked by glutaraldehyde vapors. J Mater Sci Mater Med 2002;13(1):119–23.

- [20] Li L, Beniash E, Zubarev ER, Xiang W, Rabatic BM, Zhang G, et al. Assembling a lasing hybrid material with supramolecular polymers and nanocrystals. Nat Mater 2003;2(10):689–94.
- [21] Wang CC, Lu JN, Young TH. The alteration of cell membrane charge after cultured on polymer membranes. Biomaterials 2007;28(4):625–31.
- [22] Valli M, Leonardi L, Strocchi R, Tenni R, Guizzardi S, Ruggeri A, et al. "In vitro" fibril formation of type I collagen from different sources: biochemical and morphological aspects. Connect Tissue Res 1986;15(4):235–44.
- [23] Stuart K, Panitch A. Influence of chondroitin sulfate on collagen gel structure and mechanical properties at physiologically relevant levels. Biopolymers 2008;89(10):841–51.
- [24] Cope AP. Methods in Molecular Medicine 135. Arthritis Research Methods and Protocols, vol. 1. Totowa, NJ: Humana Press; 2007.
- [25] Forouzandeh F, Jalili RB, Hartwell RV, Allan SE, Boyce S, Supp D, et al. Local expression of indoleamine 2,3-dioxygenase suppresses T-cell-mediated rejection of an engineered bilayer skin substitute. Wound Repair Regen 2010;18(6):614–23.
- [26] Liang WH, Kienitz BL, Penick KJ, Welter JF, Zawodzinski TA, Baskaran H. Concentrated collagen-chondroitin sulfate scaffolds for tissue engineering applications. J Biomed Mater Res A 2010;94(4):1050–60.
- [27] Li M, Moeen Rezakhanlou A, Chavez-Munoz C, Lai A, Ghahary A. Keratinocyte-releasable factors increased the expression of MMP1 and MMP3 in co-cultured fibroblasts under both 2D and 3D culture conditions. Mol Cell Biochem 2009;332(1/2):1–8.
- [28] Sarti B, Scandola M. Viscoelastic and thermal properties of collagen/poly(vinyl alcohol) blends. Biomaterials 1995;16(10):785–92.
- [29] Nilasaroya A, Poole-Warren LA, Whitelock JM, Jo Martens P. Structural and functional characterisation of poly(vinyl alcohol) and heparin hydrogels. Biomaterials 2008;29(35):4658-64.
- [30] Heng TS, Dudakov JA, Khong DM, Chidgey AP, Boyd RL. Stem cells meet immunity. J Mol Med 2009;87(11):1061–9.
- [31] Nuttelman CR, Mortisen DJ, Henry SM, Anseth KS. Attachment of fibronectin to poly(vinyl alcohol) hydrogels promotes NIH3T3 cell adhesion, proliferation, and migration. J Biomed Mater Res 2001;57(2):217–23.
- [32] Ballios BG, Cooke MJ, van der Kooy D, Shoichet MS. A hydrogel-based stem cell delivery system to treat retinal degenerative diseases. Biomaterials 2010;31(9):2555-64.
- [33] Pederson AW, Ruberti JW, Messersmith PB. Thermal assembly of a biomimetic mineral/collagen composite. Biomaterials 2003;24(26):4881–90.
- [34] Alina Sionkowska JS, Marcin Wisniewski. Photochemical stability of collagen/ poly(vinylalcohol) blends. Polym Degrad Stability 2004;83:117–25.
- [35] Barbani N, Cascone MG, Giusti P, Lazzeri L, Polacco G, Pizzirani G. Bioartificial materials based on collagen: 2. Mixtures of soluble collagen and poly(vinylalcohol) cross-linked with gaseous glutaraldehyde. J Biomater Sci Polym Ed 1995;7(6):471–84.
- [36] Silver Frederick H, Freeman Joseph SGP, Devore Dale W. Viscoelastic properties of young and old human dermis: a proposed molecular mechanism for elastic energy storage in collagen and elastin. J Appl Polym Sci 2002:86(8):1978–85.
- [37] Eming SA, Whitsitt JS, He L, Krieg T, Morgan JR, Davidson JM. Particle-mediated gene transfer of PDGF isoforms promotes wound repair. J Invest Dermatol 1999:112(3):297-302.
- [38] Zahouani H, Pailler-Mattei C, Sohm B, Vargiolu R, Cenizo V, Debret R. Characterization of the mechanical properties of a dermal equivalent compared with human skin in vivo by indentation and static friction tests. Skin Res Technol 2009;15(1):68-76.
- [39] Bader DL, Bowker P. Mechanical characteristics of skin and underlying tissues in vivo. Biomaterials 1983;4(4):305–8.
- [40] Linge C, Richardson J, Vigor C, Clayton E, Hardas B, Rolfe K. Hypertrophic scar cells fail to undergo a form of apoptosis specific to contractile collagen-the role of tissue transglutaminase. I Invest Dermatol 2005:125(1):72–82.
- [41] Ko CS, Huang JP, Huang CW, Chu IM. Type II collagen-chondroitin sulfatehyaluronan scaffold cross-linked by genipin for cartilage tissue engineering. J Biosci Bioeng 2009;107(2):177–82.
- [42] Barrett AJ, Knight CG, Brown MA, Tisljar U. A continuous fluorimetric assay for clostridial collagenase and Pz-peptidase activity. Biochem J 1989;260(1):259–63.
- [43] Eberli D, Rodriguez S, Atala A, Yoo JJ. In vivo evaluation of acellular human dermis for abdominal wall repair. J Biomed Mater Res A 2010;93(4):1527–38.
- [44] Prasertsung I, Kanokpanont S, Bunaprasert T, Thanakit V, Damrongsakkul S. Development of acellular dermis from porcine skin using periodic pressurized technique. J Biomed Mater Res B Appl Biomater 2008;85(1):210–9.